Distinct Concentration-Dependent Effects of the Polo-like Kinase 1–Specific Inhibitor GSK461364A, Including Differential Effect on Apoptosis

Aidan G. Gilmartin, Maureen R. Bleam, Mark C. Richter, Symon G. Erskine, Ryan G. Kruger, Lenore Madden, Daniel F. Hassler, Gary K. Smith, Richard R. Gontarek, Mary P. Courtney, David Sutton, Melody A. Diamond, Jeffrey R. Jackson, and Sylvie G. Laquerre

GlaxoSmithKline Pharmaceuticals, Collegeville, Pennsylvania

Abstract

Polo-like kinase 1 (Plk1) is a conserved serine/threonine kinase that plays an essential role in regulating the many processes involved in mitotic entry and progression. In humans, Plk1 is expressed primarily during late G_2 and M phases and, in conjunction with Cdk1/cyclin B1, acts as master regulatory kinases for the myriad protein substrates involved in mitosis. Plk1 overexpression is strongly associated with cancer and has been correlated with poor prognosis in a broad range of human tumor types. We have identified a potent, selective, reversible, ATP-competitive inhibitor of Plk1, GSK461364A, capable of inhibiting cell growth of most proliferating cancer cell lines tested. We observe distinct cell cycle effects of GSK461364A depending on the dose used. The predominant phenotype for cells treated with GSK461364A is prometaphase arrest with characteristic collapsed polar *polo* spindle. At high concentrations, GSK461364A delays mitotic entry in G_2 followed by gradual progression into terminal mitosis; in some cell lines, this correlates with decreased apoptosis. Cell culture growth inhibition by GSK461364A can be cytostatic or cytotoxic but leads to tumor regression in xenograft tumor models under proper dose scheduling. Finally, we describe pharmacodynamic biomarkers of GSK461364A activity (pHH3 and Plk1) that are currently being evaluated in human cancer clinical trials. [Cancer Res 2009;69(17):6969–77]

Introduction

Agents targeting microtubule dynamics, such as taxanes and *Vinca* alkaloids, are widely used in the clinic against multiple types of cancer. However, they carry substantial liabilities such as significant and variable dose-limiting toxicities. The potential for new selective drugs to target alternative mitotic mechanisms offers the possibility not only to overcome certain limitations of current tubulin-targeted antimitotic drugs but to expand the scope of clinical efficacy that those drugs have established (1). The serine/threonine Polo-like kinase 1 (Plk1) represents a compelling mitotic target due to its multiple roles at key steps of mitosis and its involvement in cancer progression. Plk1 plays a role in mitotic entry (2–5), centrosome maturation and chromosome movement (6–9), direct and indirect activation of the anaphase promoting complex/cyclosome (10–13), formation of bipolar spindles, and accumulation of spindle assembly checkpoint proteins at the kinetochores (14–18). Overexpression of Plk1 is transforming (19), and several studies have shown correlations between Plk1 expression, histologic grade, and poor prognosis in various cancers (20).

Several Plk1 inhibitors (21–29) are currently under investigation in clinical trials. Here we describe the identification and characterization of the imidazotriazine GSK461364A, an inhibitor of Plk1 kinase activity. GSK461364A is an ATP competitive, highly selective Plk1 inhibitor producing mitotic arrest with the hallmark *polo* spindle morphology in tumor cells. GSK461364A inhibits cancer cell line proliferation from multiple origins with minimal toxicity in nondividing human cells. Consistent with the multiple known functions of Plk1 throughout mitosis, we observed dose-dependent differences in the nature of cell cycle arrest and the consequent cell fate. Finally we show that GSK461364A showed clear antitumor activity in human tumor xenograft models, and that the dose-dependent biological effects seen *in vitro* were recapitulated *in vivo*.

Materials and Methods

Enzyme assays. Kinase reactions were performed in a final assay volume of 10 μL using the Z′-Lyte Assay kit (Ser/Thr peptide 16, Invitrogen). Briefly, reactions contained 50 mmol/L HEPES (pH 7.5), 10 mmol/L $MgCl_2$, 1 mmol/L EGTA, 1 mmol/L DTT, 0.01% Brij 35, 0.01 mg/mL casein, 200 μmol/L ATP, 200 μmol/L Polo Box peptide (NH2-MAGPMQS[pT]PLNGAKK-OH, 21st Century Biochemicals), and 6 nmol/L recombinant Plk1 (H6-tev-PLK 1-603, GlaxoSmithKline). Plk1 was preincubated for 60 min in the presence or absence of 0 to 1,000 nmol/L GSK461364A (GlaxoSmithKline). Reactions were then initiated by the addition of 2 μmol/L peptide. After 15 min at 23°C, reactions were quenched and processed according the Z′-Lyte protocol and read on an EnVision plate reader. Raw fluorescence values were converted to concentration of product formed using substrate and product standards. IC_{50} values were determined using a two-parameter fit (Hill coefficient and IC_{50}) using GraFit software (Erithacus). Because the potency of inhibition for GSK461364A was observed to vary as a function of the ATP concentration in a manner consistent with an ATP-competitive mode of inhibition (data not shown), an upper limit for the K_i^{*app} for GSK461364A was determined by applying the Cheng-Prusoff relationship for a competitive inhibitor (ref. 30; ATP K_m^{*app} = 16 μmol/L) to the IC_{50} value obtained with 60 min preincubation of GSK461364A.

Plk scintillation proximity assays. Full-length Plk1 (Cell Signaling) assays were performed as described (31) with minor changes. The enzyme activity was measured in a reaction buffer containing 25 mmol/L HEPES (pH 7.2), 15 mmol/L $MgCl_2$, 1 μmol/L ATP, 0.2 μCi/well [γ-^{33}P]ATP (10 Ci/mmol), 1 μmol/L substrate peptide (Biotin-Ahx-SFNDTLDFD: from 21st Century Peptides), 0.15 mg/mL bovine serum albumin, 1 mmol/L DTT,

Note: Supplementary data for this article are available at Cancer Research Online (http://cancerres.aacrjournals.org/).

Requests for reprints: Aidan G. Gilmartin, GlaxoSmithKline, 1250 S. Collegeville Road, Collegeville, PA 19426. Phone: 610-917-4078; Fax: 610-917-4181; E-mail: Aidan.G.Gilmartin@GSK.com.

doi:10.1158/0008-5472.CAN-09-0945

and 12.5 nmol/L full-length Plk1. Reactions were performed at room temperature in total volume of 20 μL using white 96-well plates. After 120 min, 100 μL of stop mix [33 mmol/L EDTA, 3.0 mg/mL streptavidin scintillation proximity assay (SPA) beads (GE Healthcare Life Sciences) PBS, 50 μmol/L ATP] were added to each well and left for 20 min. Aliquots (100 μL) were then transferred to GF/C filter plates, and the beads were washed four times with 100 μL PBS solution using vacuum filtration. Plates were sealed and placed in a Packard TopCount (GMI, Inc.) running a standard ^{33}P SPA protocol reading each well for 60 s. Percentage inhibition was then calculated relative to control reactions containing either no inhibitor (signal max) or 50 mmol/L EDTA (background).

Kinase selectivity assays. To determine the kinase selectivity of GSK461364A, the inhibition of 48 recombinant protein kinases was characterized at GlaxoSmithKline according to standard biochemical procedures. As much as possible, the assays were configured so that the IC_{50} values approximate the intrinsic binding constant (K_i or K_d) of GSK461364A to each enzyme and can therefore be compared for selectivity against these kinases. However, the selectivity in cells may be different because inhibitor potency will be affected to differing degrees based on the ATP K_m values for each kinase.

Cell culture, proliferation assay, and caspase activity assay. Cell lines were obtained from American Type Culture Collection and grown in the recommended media at 37°C, 5% CO_2 in a humidified incubator. Cells were plated in triplicate 96-well microtiter plates at 1,000 cells per well in culture media. GSK461364A dissolved in DMSO or negative control (0.1% DMSO) were added the following day, and one plate was harvested with 50 μL of CellTiter-Glo (Promega) for a time 0 (T = 0) measurement. Remaining duplicate cell plates were typically incubated for 72 h. Cells were then lysed with 50 μL CellTiter-Glo, and chemiluminescent signal was read on the Wallac EnVision 2100 plate reader. All data were normalized to signal at time of compound addition (T = 0). Curves were analyzed using the XLfit (IDBS Ltd.) curve-fitting tool for Microsoft Excel to determine the gI_{50} (concentration of 50% growth inhibition relative to T = 0 and Y_{max} values), the gI-maximum (concentration giving maximum growth inhibition), and the Y_{min} (bottom of the four-parameter curve at gI-maximum). Based on Y_{min} value, we defined the maximum biological response for each cell line as "cytotoxic" (a Y_{min} < 100% reflecting a net-cell decrease), "cytostatic" (Y_{min} = 100–200%, wherein cells undergo one or fewer complete divisions), or "resistant" (Y_{min} > 200%). For measure of caspase-3/caspase-7 activity, cells were prepared and treated as above but were then harvested with 100 μL of CaspaseGlo (Promega) and chemiluminescent signal read as above.

Immunocytochemistry. Cells treated with GSK461364A in cell culture slides (NalgeNunc) were fixed first with 3.7% formaldehyde in Dulbecco's PBS (without Ca/Mg) and then with −20°C methanol with several PBS washes in between. Cells were permeablized with 0.1% Triton X-100 in PBS. Nonspecific binding was blocked by incubating for 30 min at 37°C with 5% normal donkey serum (Jackson) in PBS (blocking buffer). A primary antibody mixture of mouse anti–γ-tubulin (Abcam AB11316) and rabbit anti–α-tubulin (Abcam AB15246) was added in blocking buffer and allowed to bind overnight at 4°C. After several washes with blocking buffer, 4′,6-diamidino-2-phenylindole (DAPI; Vector Laboratories) and secondary antibodies rhodamine red-donkey anti-mouse IgG and CY2-donkey anti-rabbit IgG (Jackson) were added in blocking buffer for 30 min at room temperature. After additional washes, coverslips were mounted with anti-fade medium (Invitrogen). Microscopy was performed using an Olympus IX71 fluorescent microscope under the 60× oil objective. Images were captured and analyzed with Image-Pro Plus 5.1 software.

Phosphorylated histone H3 (Ser^{10}; pHH3) ELISA. Briefly, 96-well ELISA plates (Corning) were coated with 2.5 μg/mL anti-Pan histone (Millipore) capture antibody in PBS (with Ca/Mg) overnight at 4°C. Plates were then blocked with 5% nonfat dry milk (Carnation) for 1 h at room temperature and then washed repeatedly with PBS containing 0.05% Tween 20 (PBST). Cells treated with GSK461364A in 96-well microtiter plates (Nunc) were lysed at room temperature for 30 min with CelLytic-M Cell Lysis Reagent (Sigma) containing 100 nmol/L calyculin A, 1 mmol/L sodium fluoride, 1 mmol/L sodium orthovanadate, 20 μg/mL DNase I (Roche), and 1× EDTA-free protease inhibitor tablets (Roche). Lysates were transferred to the ELISA plates and allowed to bind for 1 h at room temperature. Plates were washed, and the anti-pHH3 (Ser^{10}; Abcam) detection antibody was applied at 1:1,000 in 1% nonfat dry milk/PBST. After 2 h of room temperature incubation and wash, the secondary antibody was applied (1:1000) for 1 h at room temperature. The plates were washed again, and BM POD (Roche Applied Science) chemiluminescent substrate was added. Luminescent signal was detected on the Wallac EnVision 2100 plate reader (Perkin-Elmer).

Immunohistochemistry. Tissue from Colo205 tumor xenograft model was harvested at 24 and 48 h postdose with GSK4613464A or vehicle. Tumor tissue cut to ~100 mm^3 samples was fixed in 10% formalin (neutral-buffered, VWR; VW3239-7) for 24 h and then transferred to 70% ethanol before paraffin embedding. Paraffin-embedded blocks were sectioned to 6 μm. Sections were rehydrated, and an antigen retrieval step was incorporated to improve detection of pHH3 (3-min microwave of slides immersed in 10 mmol/L citrate buffer, pH 6.0). Antibodies were pHH3 (Ser^{10}; Upstate Biotech, 06-570), Plk1 (Calbiochem, 35-206), and Ki-67 (DAKO, MIB-1), and DNA was counterstained with hematoxylin. Sectioned slides were shipped to Mosaic Laboratories for staining, imaging, and quantitation.

DNA content analysis. Cells were treated with serial dilutions of GSK461364A for 24 h, fixed in chilled 70% ethanol for 2 h, washed with PBS, and stained with a propidium iodide (Molecular Probes) solution containing 20 μg/mL propidium iodide, 0.2 mg/mL Rnase A, and 0.1% Triton X-100 in PBS. Data were acquired on a FACSCalibur and analyzed with the FlowJo software package (Tree Star, Inc.).

Cyclin B1-GFP U2OS cell line. The stable cyclin B1-GFP expressing U2OS cell line was obtained from GE Healthcare Life Sciences. The cell line encodes a fused cyclin B1-GFP protein under the cyclin B1 promoter, which defines the phase of individual cells in the cell cycle based on cell cycle–dependent expression, destruction, and localization of cyclin B1-GFP fusion protein. Cells were treated with serial dilutions of GSK461364A for 24 to 72 h, counterstained with the DNA dye Draq5, and imaged and analyzed with the In Cell Analyzer 3000 (GE).

Tumor xenograft studies. Cells were implanted in Nude mice and grown as tumor xenografts. Dosing began when tumors achieved ~100 mm^3. GSK461364A or the vehicle [4% DMA/Cremaphore (50:50), pH 5.6] was given i.p. to mice every 2 d (q2dx6, q2dx12) or every 4 d (q4dx3) at nominal dose levels of 25, 50, and 100 mg/kg/dose. Results are reported as median tumor volume for n = 7 to 8 mice. Paclitaxel (Mead Johnson; 30 mg/kg i.v.; q4dx3) was used as a positive control for comparison. Tumors were measured thrice a week with Vernier calipers, and tumor volume was calculated from two-dimensional measurements using an equation approximating the volume of a prolate ellipsoid [tumor volume mm^3 = (length × width^2) × 0.5]. The maximum tolerated dose was defined as the highest dose that produced >20% mortality or >20% weight loss (~4 g). Antitumor activity was defined as tumor growth delay (TGD), partial regression (PR), or complete regression (CR). TGD represents the time differential between the treated and control tumors to reach a predetermined tumor volume of 1,000 mm^3. PR was defined as a decrease in an individual tumor volume to one-half the initial starting volume for at least 1 wk (three consecutive measurements). CR was defined as a decrease in an individual tumor volume to <13 mm^3 for at least 1 wk.

Results

Identification and biochemical characterization of GSK461364A. GSK461364A was identified after a library screening campaign using a Plk1 scintillation proximity assay, accompanied by lead optimization of the identified chemical entity (structure/activity relationship), leading to the identification of GSK461364A (32). When evaluated against full-length Plk1 in an *in vitro* biochemical assay, inclusion of a 60-minute preincubation step significantly increased the compound potency (Supplementary Fig. S1), suggesting a time-dependent mechanism of inhibition with an apparent dissociation constant (K_i^{*app}) value of <0.5 ± 0.1 nmol/L (Supplementary Table S1). Upon rapid dilution of a preformed

enzyme-inhibitor complex into a substrate mix with saturating ATP, a qualitatively slow recovery of activity was observed (data not shown), indicating that the dissociation of the compound was reversible although not instantaneous and confirming the observed time-dependent inhibition. These data also confirm that the true potency for Plk1 could be substantially lower than the K_i^{*app} determined above.

When evaluated against Plk2 and Plk3 (Supplementary Table S1), GSK461364A was significantly less potent (K_i^{*app}: 860 and 1,000 nmol/L, respectively). To further explore selectivity, GSK461364A was tested against an in-house panel of 48 kinases. GSK461364A had at least 1,000-fold selectivity for Plk1 over the majority of kinases tested (Supplementary Fig. S2). GSK461364A was further screened against a commercial panel of recombinant kinases (KinaseProfiler, Millipore). In this screen, 37 of 262 kinases showed >50% inhibition with only six kinases inhibited by >90% at 10 μmol/L (>5,000-fold of the IC_{50} for Plk1; Supplementary Table S2). Taken together, these data show that GSK461364A is a potent, selective, reversible, ATP-competitive inhibitor of Plk1 with a prolonged rate of dissociation from the enzyme.

GSK461364A causes prometaphase arrest *in vitro*. To study the consequence of GSK461364A exposure on cell cycle, a NSCLC line A549 was treated with serial dilutions of GSK461364A for 20 hours and propidium iodide stained, and DNA content was analyzed by flow cytometry (Fig. 1*A*). Concentrations at above 10 nmol/L GSK461364A caused increased 4N DNA content indicating G_2-M arrest. With extended exposure duration, increased sub-2N DNA indicating increased cell death is observed for GSK461364A concentrations of >10 nmol/L (data not shown).

The mitotic phenotype caused by this Plk1 inhibitor was confirmed by cell staining. A549 cells treated for 16 hours with GSK461364A were fixed and immunostained for α-tubulin, γ-tubulin, and DAPI. At 20 nmol/L GSK461364A (approximately gI_{50}), a significant increase in mitotic cells is evident. At this relatively low active concentration, mitotic cells exhibit a mixture of aberrant bipolar and monopolar spindles (Fig. 1*B*). Where cells exhibit bipolar centrosomal separation, chromatin is incompletely aligned at the metaphase plate. For these cells, γ-tubulin staining at the centrosomes is evident but relatively reduced. At higher concentration GSK461364A (313 nmol/L; approximately gI-maximum), we observed primarily monopolar/apolar spindles with no evident γ-tubulin staining at centrosomes. Notably, chromatin is not organized in a rosette around the monopolar spindle (characteristic of the KSP\Eg5 inhibitor monastrol), suggesting a lack of syntelic microtubule-kinetochore attachments; instead, the chromatin is highly condensed and disorganized around the aberrant mitotic spindle. In addition, DAPI staining shows significant micronucleation in those cells that survived mitotic arrest and underwent aberrant mitotic exit with tetraploidy, termed mitotic slippage (Fig. 1*C*). With prolonged drug treatment, micronucleation is observed in virtually all surviving cells.

GSK461364A broadly inhibits cancer cell proliferation with differential survival outcome. In a proliferation assay, GSK461364A causes cell growth inhibition in a majority of the 74 tested cancer cell lines. In this assay, a measurement was performed at the time of compound addition (T = 0) and after 72 hours drug incubation. Results (Fig. 2) show that 89% of cell lines (66 of 74 lines) responded to GSK461364A with a gI_{50}

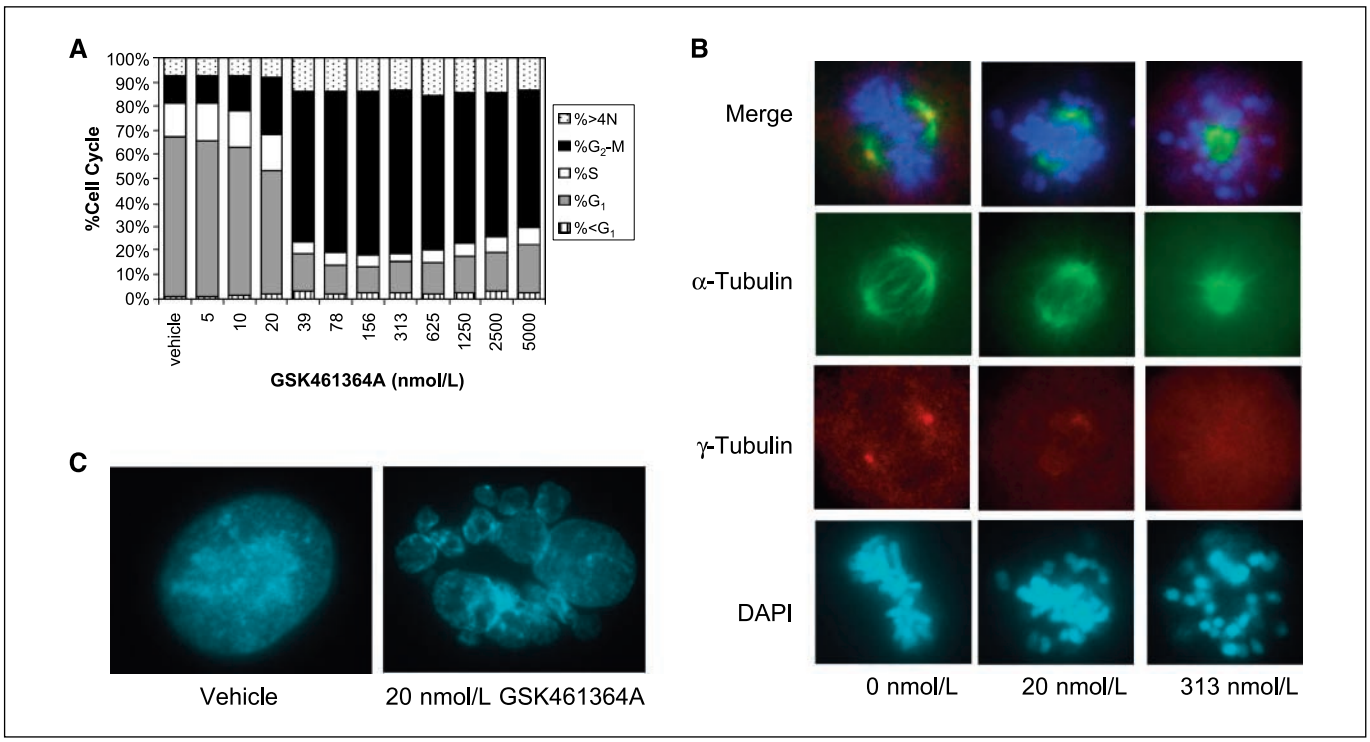

Figure 1. Plk1 inhibitor GSK461364A causes aberrant mitotic arrest and micronucleation. *A,* A549 lung carcinoma lines were treated for 20 h with serial dilutions of GSK461364A, and DNA content was analyzed by flow cytometry propidium iodine staining. GSK461364A at concentrations of >20 nmol/L blocks cells in G_2-M phase with reduction of cells in G_1 phase. Maximum G_2-M arrest is observed at concentrations of ≥39 nmol/L. *B,* A549 cells were treated for 16 h with different concentrations of GSK461364A and analyzed by immunofluorescence for α-tubulin (*green*), γ-tubulin (*red*), and chromatin (DAPI; *blue*). GSK461364A causes mitotic arrest at concentrations of 20 nmol/L with mitotic spindle aberrations at higher concentrations of 313 nmol/L. These aberrations were principally in the form of spindle monopolarity and chromatin disorganization. *C,* micronucleation is evident at ≥20 nmol/L GSK461364A by DAPI staining.

(concentration required to inhibit 50% cell growth) of ≤100 nmol/L. Notably, although the rate of cell doublings did not generally show strong correlation with gI_{50} values, cell lines that exhibited almost no cell growth during the 72-hour assay did show correspondingly little effect from GSK461364A exposure (data not shown). A comparison of human umbilical vascular endothelial cells cultured in subconfluent or confluent nondividing conditions confirms that cell division is necessary for the activity of GSK461364A (Supplementary Fig. S3), in that there is no apparent toxicity on human normal nonproliferating cells.

A comparison of the maximum drug effect (Y_{min} of the four-parameter growth inhibition curve) normalized to $T = 0$ value allows a useful determination of the relative cytotoxic or cytostatic outcome GSK461364A caused for a given cell line. Broadly, we considered a Y_{min} of <100% to reflect a net cell decrease indicating population cytotoxicity; similarly we defined cytostasis as Y_{min} = 100% to 200%, wherein cells undergo one or fewer complete divisions. Data show (Fig. 2; Supplementary Table S3) that at maximum effective drug concentrations 42% of cell lines treated with GSK461364A had net cytotoxicity, 45% had net cytostatic response, and 13% showed cell growth greater than 1 doubling (Y_{min} > 200%). These results show that GSK461364A potently inhibits cell proliferation of multiple cancer cell lines, but that survival outcomes can vary depending on the individual cell line tested. Whereas this method of binning cell response in cultured cells clearly indicates differences in outcome, its utility for predicting *in vivo* efficacy is limited: essentially all tumor xenograft models tested showed degrees of tumor growth inhibition (Fig. 5*D*), but the degrees did not correlate strongly with the *in vitro* binning. However, it is worth noting that among the xenograft tumor lines, those with the most cytotoxic response in cell culture (least Y_{min}), MDA-MB-231 and Colo205, also had the largest TGD, and conversely the most resistant cells (greatest Y_{min}), MX-1, had the smallest TGD.

GSK461364A blocks cells in G_2 and M phases of the cell cycle and causes M-phase caspase-3/caspase-7 activation. Whereas GSK461364A results in a normal sigmoidal dose-response curve on many cancer cell lines (40%), many other cell lines (60%), such as the human breast cancer ZR-75-1 cells, respond to Plk1 inhibitor GSK461364A in a biphasic manner (Fig. 3*A*). Cell lines with a biphasic response pattern exhibit maximum growth inhibition at "low-active" drug concentrations between 10 and 250 nmol/L but

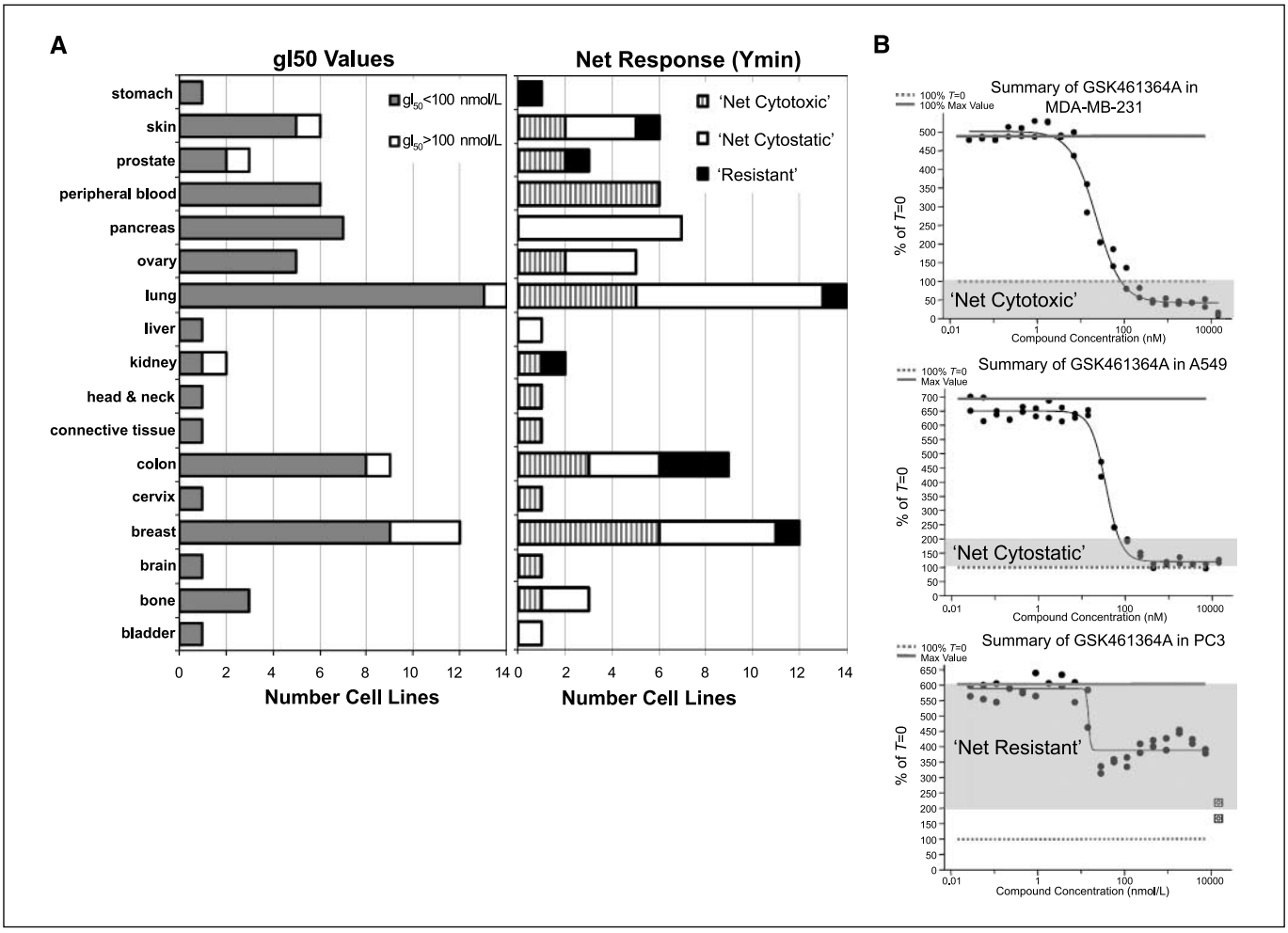

Figure 2. Activity of Plk1 inhibitor on cancer cell lines from different tissue of origin. *A,* GSK461364A activity was tested against 74 cancer cell lines from different tissues of origin using a 72-h growth assay. Sensitivity to Plk1 inhibitor was segregated by gI_{50} (greater or less than 100 nmol/L) and by the maximum net cell change (defined by the Y_{min} of a four-parameter-fit curve) relative to the $T = 0$ starting population: cytotoxic (Y_{min} < 100%, $T = 0$), cytostatic (Y_{min} = 100–200%, $T = 0$), or resistant (Y_{min} > 200%, $T = 0$). *B,* examples of the alternative net responses are shown for MDA-MB-231, A549, and PC3 cell lines; $T = 0$ and Y_{max} values are indicated with dotted and solid gray lines, respectively.

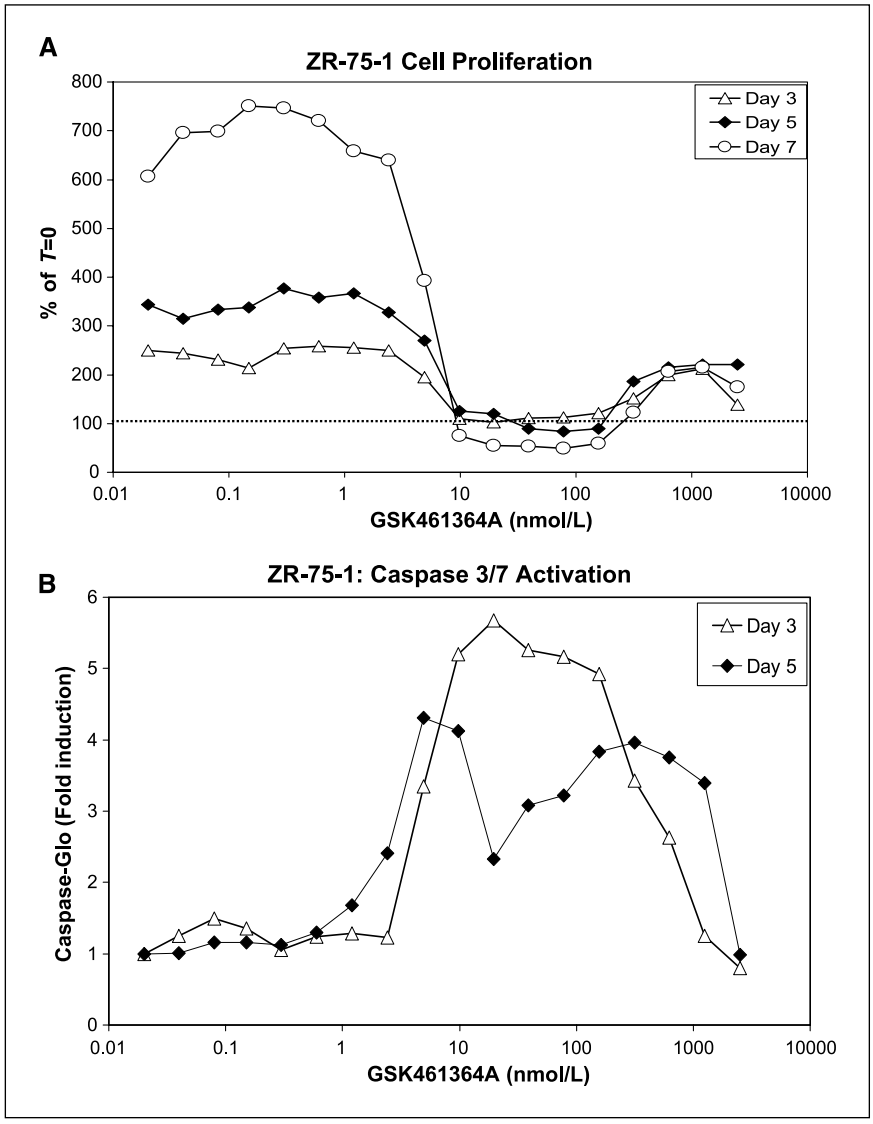

Figure 3. Concentration and time-dependent growth inhibition and caspase-3/caspase-7 activation by GSK461364A. ZR-75-1 breast cancer cell lines were treated with GSK461364A at different concentrations and quantitated for cell number (CellTiter-Glo, *A*) and caspase-3/caspase-7 activation (CaspaseGlo, *B*) at different time points. At low-active (10–250 nmol/L) and high-active (>250 nmol/L) concentrations of Plk1 inhibitor, different biological outcomes are evident. On day 3, caspase activation and growth inhibition are maximally observed at 10 to 250 nmol/L GSK461364A; >250 nmol/L GSK461364A results in reduced apoptosis and a residual viable but nondividing cell population. Prolonged drug treatment of 5 to 7 d results in some increased caspase activation at the high-active drug concentrations.

seem to have a residual viable cell population at "high-active" concentrations of >250 nmol/L. Furthermore, caspase-3/caspase-7 is maximally activated at a low-active concentration of GSK461364A corresponding to maximal growth inhibition (Fig. 3*B*). Notably, the viable cells at high-active concentrations do not seem to grow beyond one cell division (200% of $T = 0$) assaying out to 7 days. These data suggest GSK461364A dose-dependent differences in outcome due to extent of Plk1 inhibition, with maximum apoptosis resulting from low-active drug concentrations.

To further investigate this concentration-dependent outcome to Plk1 inhibition, we used an engineered U2OS (osteosarcoma) cell line expressing a fused cyclin B1-GFP protein under the cyclin B1 promoter in which the G_2 and M phases can be differentiated using an image-based analysis. After 24 h of exposure to GSK461364A, cells were blocked primarily in mitosis and, to a lesser extent, in G_2 at low-active concentrations of GSK461364A (10–250 nmol/L; Fig. 4*A*). However, at increasing GSK461364A concentration (>250 nmol/L) the percentage of G_2 cells exceeds the percentage of mitotic cells. Notably by 48 hours, the majority of cells at the high-active concentrations are mitotic (Fig. 4*B*), suggesting that the G_2 delay is transient, preceding mitotic progression and arrest.

To confirm that this concentration-dependent cell cycle arrest was not unique to U2OS cells, analysis was performed on additional cell lines detecting levels of phosphorylated histone H3 (Ser^{10}; pHH3) as a biomarker for mitosis. U2OS, A549, HT29 (colon cancer), and MDA-MB-468 (breast cancer) cell lines were treated for 19 hours with serial dilutions of GSK461364A and pHH3 levels measured by ELISA. In each cell line, the level of pHH3 peaked at low-active concentrations GSK461364A (10–250 nmol/L) and then decreased slightly at higher concentrations (Fig. 4*C*). These results support the conclusion that the predominant effect of GSK461364A is mitotic arrest but that at sufficiently high concentrations GSK461364A may delay entry into mitosis. This G_2 delay seems to be transient and in the short-term may be protective from apoptosis.

GSK461364A is efficacious in xenograft tumor models. GSK461364A was dosed i.p. in mice bearing Colo205 (colorectal) xenograft tumors, and several dosing schedules were tested (Fig. 5). Higher intermittent dosing with a q4dx3 (one dose every 4 days repeated thrice) schedule at 100 mg/kg (Fig. 5*A*) resulted in 18 days TGD and one PR out of five mice treated. More frequent lower dosing with 50 mg/kg q2dx6 schedule (Fig. 5*B*) resulted in longer

TGD (39 days) and 2PR. Extending the schedule of 50 mg/kg q2dx12 resulted in longer TGD (62 days) with one CR and 3PR observed (Fig. 5*C*), efficacy approaching the antitumor activity of the positive control agent paclitaxel. On the q2d treatment schedules, 100 mg/kg were not tolerated after the third drug treatment (with >15% body weight loss and mortality of two of five mice). For all schedules of GSK461364A, tumors decreased in mass during the treatment period, but tumor growth resumed upon cessation of treatment. The optimal dosing schedule of 50 mg/kg q2dx12 showed various degrees of TGD in multiple xenograft tumor models tested (Fig. 5*D*).

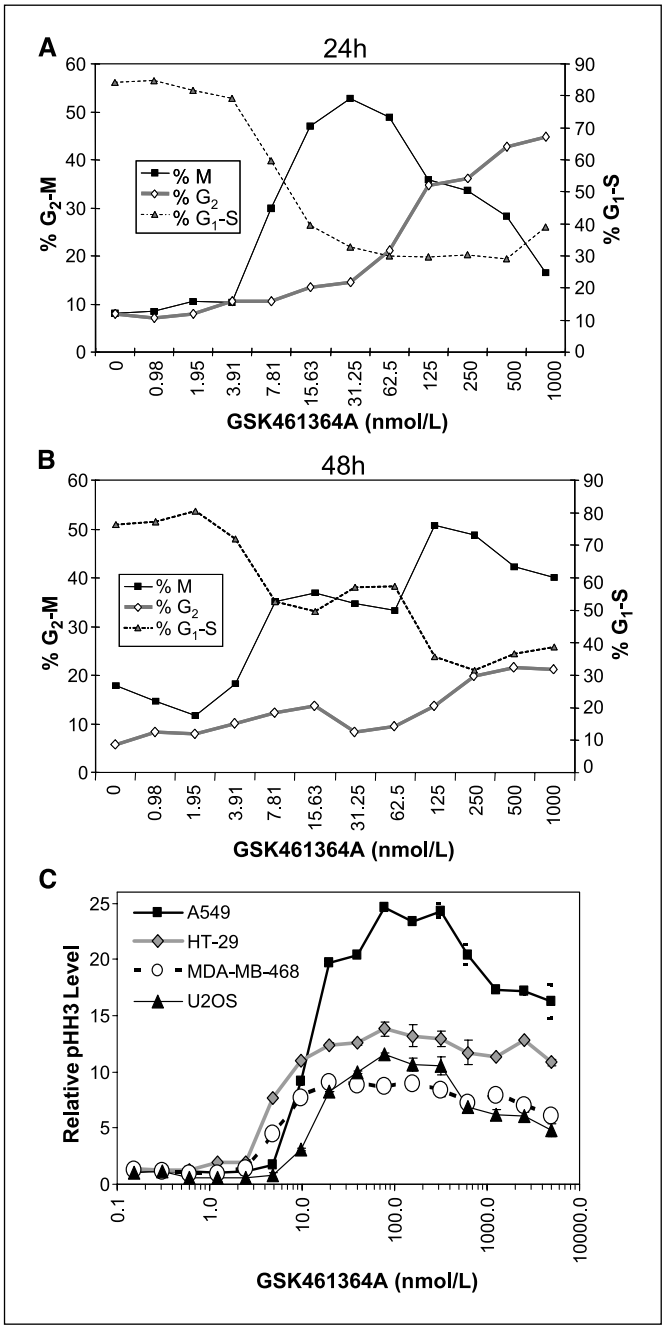

Figure 4. Plk1 inhibitor GSK461364A causes mitotic arrest at low concentrations and G_2 delay at high concentrations. An engineered U2OS cell line encoding a fused cyclin B1-GFP protein under the cyclin B1 promoter was used to define the phase of individual cells in the cell cycle based on cell cycle–dependent expression, destruction, and localization of cyclin B1-GFP fusion protein after treatment with Plk1 inhibitor GSK461364A. *A,* after a 24-h treatment, cells are blocked in mitosis at low concentration of Plk1 inhibitor (10–100 nmol/L) and in G_2 at >250 nmol/L. *B,* after a 48-h treatment, a concentration of >500 nmol/L cells progressed from G_2 block to M phase of cell cycle. *C,* various cancer cell lines were treated for 19 h with Plk1 inhibitor at different concentrations and harvested, and phosphorylated histone H3 (Ser^{10}, pHH3) levels measured by ELISA. Maximum level of pHH3 is generally observed at mid-dose of GSK461364A (10–100 nmol/L), indicating M-phase arrest. At higher concentrations, pHH3 levels are relatively lower, suggesting elevated G_2 phase arrest.

To confirm that the efficacy observed in xenograft tumor models was due to Plk1 inhibition, tumors from animals treated with GSK461364A were harvested at 24 and 48 hours posttreatment and evaluated immunohistochemically for pharmacodynamic biomarkers of mitotic arrest pHH3 (phosphorylated during M phase) and Plk1 (expressed primarily during late G_2 and M phases) and counterstained for proliferative biomarker Ki67. Ki67 was unchanged after a short-term Plk1 inhibitor treatment (Fig. 6*A*). As expected, GSK461364A at 50 and 100 mg/kg resulted in significant increases in cells positive for the mitotic analytes pHH3 and Plk1. At the efficacious dose of 50 mg/kg, the levels of pHH3 and Plk1 significantly increased 24 hours posttreatment and decreased to untreated vehicle control levels by 48 hours posttreatment, confirming that the inhibitory effects of GSK461364A are reversible by 2 days posttreatment. Notably, at the 100 mg/kg dose (not tolerated on long term), the levels of pHH3 and Plk1 increased at 24 hours posttreatment but to a lesser extent than with the lower dose of 50 mg/kg treatment; however, at 48 hours postdose with 100 mg/kg, levels of pHH3 and Plk1 increased further. This delay in pHH3 increase observed for the 100 mg/kg dose was also confirmed by immunoblotting tumor lysates for pHH3 (Supplementary Fig. S4). These data suggest, as we observed in cell culture, a transient G_2-phase delay preceding mitotic arrest at a high-active dose of GSK461364A.

In addition to the dose-dependent increase in the percentage of positive cells for the mitotic analytes pHH3 and Plk1, hematoxylin staining reveals dose-dependent differences in the mitotic chromatin. Chromosome alignment at the metaphase equatorial plate is clear in mitotic cells of tumors from mice treated with vehicle, indicating a bipoloar spindle (Fig. 6*B*). Similar metaphase-aligned chromatin is evident in tissue dosed up to 50 mg/kg. However at 50 to 100 mg/kg, the predominant phenotype transitions to disorganized condensed chromatin staining consistent with "polo" spindles. These data confirm that GSK461364A is efficacious *in vivo* and may suggest that the optimal dosing schedule *in vivo* produces biological effects consistent with the low-active concentrations of GSK461364A *in vitro* wherein peak apoptosis was observed.

Discussion

We have detailed here the activity of GSK461364A, a highly specific, ATP competitive Plk1 inhibitor. Our data confirms the essential cellular function of Plk1, as the majority of proliferating cell lines tested are growth-inhibited by GSK461364A with a gI_{50} of ≤100 nmol/L. Consistent with the mechanism of action, cell lines with inherently or induced slow doubling rates were relatively insensitive to GSK461364A; furthermore, xenograft tumor models indicated that GSK461364A is most efficacious with a sustained schedule of frequent low doses. These data suggest that sustained clinical exposure may be optimal for effective antiproliferative activity of GSK461364A.

Inhibition of Plk1 has been extensively explored using a number of molecular techniques including antibody microinjection (6), antisense (33), expression of a dominant negative (34), RNA interference (35), and most recently using small molecule inhibitors of this

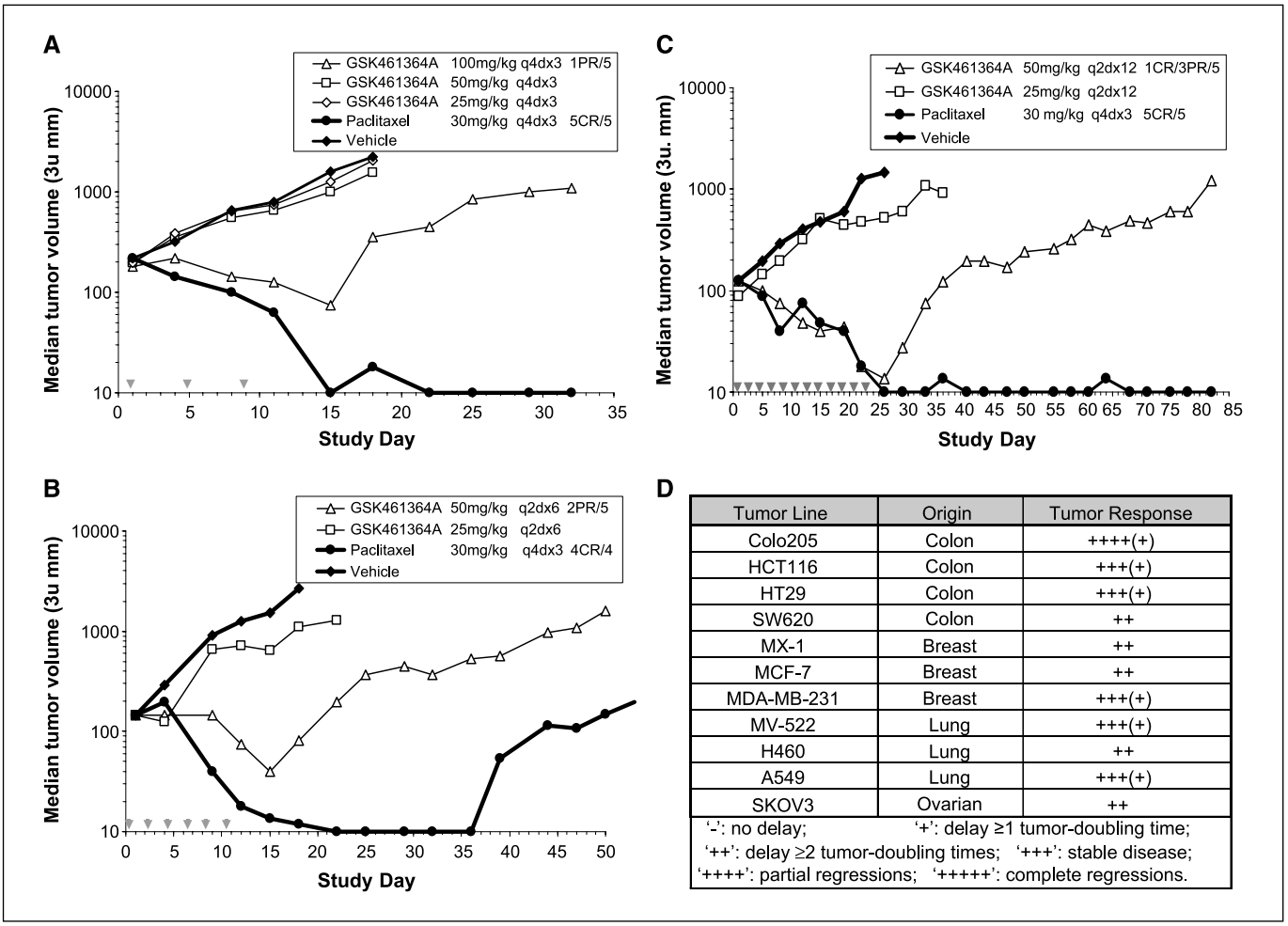

D

Tumor Line	Origin	Tumor Response
Colo205	Colon	++++(+)
HCT116	Colon	+++(+)
HT29	Colon	+++(+)
SW620	Colon	++
MX-1	Breast	++
MCF-7	Breast	++
MDA-MB-231	Breast	+++(+)
MV-522	Lung	+++(+)
H460	Lung	++
A549	Lung	+++(+)
SKOV3	Ovarian	++

'-': no delay; '+': delay ≥1 tumor-doubling time;
'++': delay ≥2 tumor-doubling times; '+++': stable disease;
'++++': partial regressions; '+++++': complete regressions.

Figure 5. GSK461364A activity in xenograft tumor models favors frequent lower dosing. TGD in Colo205 tumor model was determined for GSK461364A (i.p. administration) for q4dx3 (*A*) or q2dx6 (*B*) schedule. Extending the duration of the dosing to q2dx12 (*C*) resulted in improved antitumor activity with increased complete and PRs observed. *D,* GSK461364A was given i.p. at 25 or 50 mg/kg using a q2dx12 schedule. The maximum antitumor response is reported.

enzyme (28, 29, 31). Over time our knowledge of the number of mitotic events regulated by Plk1 and the number of Plk1 substrates has ballooned. Phosphoproteomic analysis of purified mitotic spindles alone identified 62 phosphorylation sites with the Plk1 conserved phosphorylated motif (8.4% of mapped phosphorylated sites; ref. 36). Because that study likely captured only a window of mitotic progression and only a fraction of the cell (the Taxol-stabilized mitotic spindle and associated structures), it likely underestimates the true number of mitotic phosphorylated proteins. The true number of substrates regulated by Plk1 may be far higher.

Consistent with the myriad regulatory activities attributed to Plk1 during mitosis, the biological effects of Plk1 inhibitor GSK461364A are highly dose, time, and cell line dependent. At low-active concentrations of GSK461364A (near gI_{50}) mitotic spindles accumulate with mixed bipolar and monopolar phenotypes; at higher concentrations (around gI-maximum), the predominant phenotype is mitotic arrest with characteristic "polo" monopolar (or collapsed bipolar) spindles. In these cells, microtubules radiate from unseparated centrosomes that lack γ-tubulin accumulation, and chromatin is highly condensed, ball-shaped, and disorganized around the mitotic spindle. At increasingly high concentrations (>250 nmol/L), GSK461364A induces G_2 delay in mitotic entry in some cells.

Assays measuring proliferation and apoptosis suggest that high concentrations of GSK461364A were relatively less cytotoxic compared with lower active concentrations. One hypothesis for this differential effect is that cells delayed initially in G_2 at high inhibitor concentration may trigger a stress response resulting in expression of proteins which later permit a better mitotic injury survival response. It has been shown, for example, that anti-apoptotic proteins like Bcl-XL and Bcl-2 can significantly influence survival during mitotic arrest (37, 38); expression of these or other survival proteins in G_2-delayed cells may better prepare cells to survive when they eventually enter and arrest in mitosis. Another hypothesis is that the eventual mitotic arrests observed for cells treated at higher or lower active Plk1 inhibitor concentrations differ in their injury and survivability. In this hypothesis, the transient G_2 arrest at high concentrations does not influence differential survival. Instead, when the cells eventually enter and arrest in mitosis, complete Plk1 inhibition at higher active concentration may produce a more complete early mitotic arrest, whereas partial Plk1 inhibition at lower active concentration may result in more damaging abortive attempts to progress in mitosis. We observed similar dose-dependence *in vivo*, with differences in the cell cycle phenotype in tumor xenograft models. It remains unclear whether the protective effect observed *in vitro* has

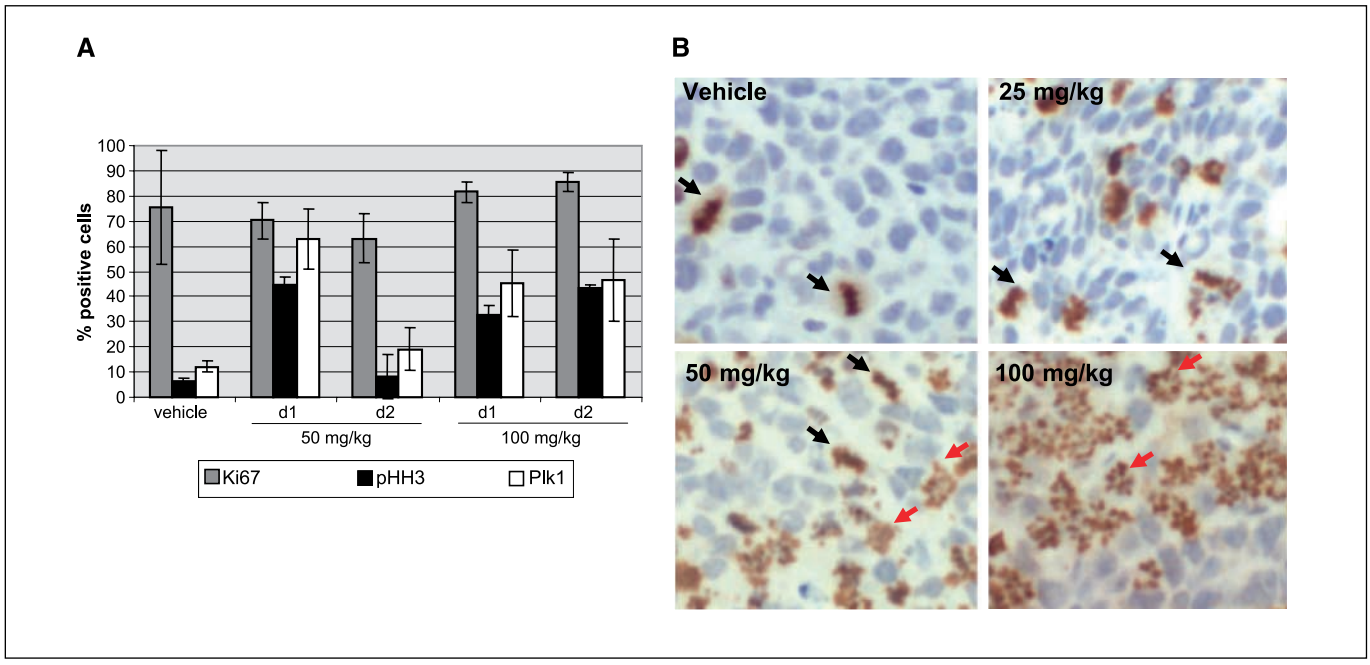

Figure 6. Immunohistochemical staining of GSK461364A-treated tumor xenografts. *A,* quantitation of immunohistochemistry shows an increase of mitotic analytes Plk1 and pHH3 at 50 mg/kg at day 1 postdosing and decrease by day 2. Notably, day 1 Plk1 and pHH3 are slightly lower at 100 mg/kg dose, but increase by day 2. Ki67 levels were unchanged. *B,* images of tumor sections from Colo205 xenografts harvested 24 h after treatment with vehicle, 25, 50, or 100 mg/kg GSK461364A. Immunohistochemical staining for pHH3 (*brown*) and hematoxylin (*blue*) shows a dose-dependent increase in mitotic cell accumulation. Chromosome alignment at the metaphase plate (*black arrows*) indicating a bipolar spindle is evident in tissue dosed up to 50 mg/kg. However, at 50 to 100 mg/kg, the predominant phenotype is disorganized chromatin staining consistent with "polo" spindles (*red arrows*).

significant effect on the ultimate outcome for the population of treated cells, but it is notable that in a Colo205 xenograft model more frequent dosing was more effective than higher intermittent dosing (for equal total doses), consistent with maximum tumor cell apoptosis occurring at intermediate active concentrations.

The complexity of investigating the effect of a Plk1 inhibitor is further complicated by the observed differences in outcome for different cell lines. Whereas 89% of the cell lines we tested showed growth inhibition with $gI_{50} \leq 100$ nmol/L, there were substantial differences across cell lines as to whether the effect was primarily cytotoxic (42%) or only cytostatic (45%). These findings agree with a recent examination of interline and intraline responses to other mitotic inhibitors including the tubulin toxins nocodazole and Taxol, and the Eg5 inhibitors monastrol and AZ138 clearly confirmed differential outcome both across cell lines and among individual cells (37). The factors affecting the differential outcome involve multiple checkpoint and apoptotic pathways. Efficacy of multiple mitotic inhibitors is generally compromised by deficiencies in the mitotic spindle assembly checkpoint (38–40). For cells that survive mitotic arrest, mitotic slippage has been shown to result in a p53/p21–dependent tetraploid G_1 arrest (termed the postmitotic checkpoint) that can affect the number of rounds of mitotic injury that cells undergo (41–43). Finally, levels of mitochondrial factors of the intrinsic apoptotic pathway including prosurvival Bcl-XL and proapoptotic Bax can significantly shift the outcome of mitotic inhibitors, tipping mitotic arrest toward apoptosis or survival (44–46). These suggest the likely complexity of predicting responsive tumor populations, but also indicate the potential for combining a Plk1 inhibitor with apoptotic potentiators currently in clinical development.

GSK461364A is broadly antiproliferative for tumor cell lines *in vitro* and efficacious in multiple *in vivo* tumor models. Use of clinical pharmacodynamic biomarkers may enable dosing patients at effective drug concentrations, potentially reducing unwanted toxicity and maximizing the antitumor activity. Finally, the use of predictive clinical biomarkers to selectively target a responsive patient population remains a highly desirable goal under ongoing investigation.

Disclosure of Potential Conflicts of Interest

No potential conflicts of interest were disclosed.

Acknowledgments

Received 3/11/09; revised 6/1/09; accepted 6/17/09; published OnlineFirst 8/18/09.

The costs of publication of this article were defrayed in part by the payment of page charges. This article must therefore be hereby marked *advertisement* in accordance with 18 U.S.C. Section 1734 solely to indicate this fact.

References

1. Jackson JR, Patrick DR, Dar MM, Huang PS. Targeted anti-mitotic therapies: can we improve on tubulin agents? [Review]. Nat Rev Cancer 2007;7:107–17.
2. Watanabe N, Arai H, Nishihara Y, Taniguchi M, Hunter T, Osada H. M-phase kinases induce phospho-dependent ubiquitination of somatic Wee1 by SCF β-TrCP. Proc Natl Acad Sci U S A 2004;101:4419–24.
3. Toyoshima-Morimoti F, Taniguchi E, Shinya N, Iwamatsu A, Nishida E. Polo-like kinase 1 phosphorylates cyclin B1 and targets it to the nucleus during prophase (vol 410, pg 215, 2001). Nature 2001;410:847–+.
4. Toyoshima-Morimoto F, Taniguchi E, Nishida E, Authors FN, Taniguchi E, Nishida E. Plk1 promotes nuclear translocation of human Cdc25C during prophase. EMBO Rep 2002;3:341–8.
5. Jackman M, Lindon C, Nigg EA, et al. Active cyclin B1-1 first appears on centrosomes in prophase. Nat Cell Biol 2003;5:143–8.
6. Lane HA, Nigg EA, Authors FN, Nigg EA. Antibody

microinjection reveals an essential role for human polo-like kinase 1 (Plk1) in the functional maturation of mitotic centrosomes. J Cell Biol 1996;135:1701–13.
7. Losada A, Hirano M, Hirano T, Authors FN, Hirano M, Hirano T. Cohesin release is required for sister chromatid resolution, but not for condensin-mediated compaction, at the onset of mitosis. Genes Dev 2002;16:3004–16.
8. Sumara I, Vorlaufer E, Stukenberg PT, et al. The dissociation of cohesin from chromosomes in prophase is regulated by polo-like kinase. Mol Cell 2002;9:515–25.
9. Gimenez-Abian JF, Sumara I, Hirota T, et al. Regulation of sister chromatid cohesion between chromosome arms. Curr Biol 2004;14:1187–93.
10. Golan A, Yudkovsky Y, Hershko A. The cyclin-ubiquitin ligase activity of cyclosome/APC is jointly activated by protein kinases Cdk1-cyclin B and Plk. J Biol Chem 2002;277:15552–7.
11. Kraft C, Herzog F, Gieffers C, et al. Mitotic regulation of the human anaphase-promoting complex by phosphorylation. EMBO J 2003;22:6598–609.
12. Moshe Y, Boulaire J, Pagano M, et al. Role of Polo-like kinase in the degradation of early mitotic inhibitor 1, a regulator of the anaphase promoting complex/cyclosome. Proc Natl Acad Sci U S A 2004;101:7937–42.
13. Hansen DV, Loktev AV, Ban KH, Jackson PK. Plk1 regulates activation of the anaphase promoting complex by phosphorylating and triggering SCF β TrCP-dependent destruction of the APC inhibitor Emi1. Mol Biol Cell 2004;15:5623–34.
14. van Vugt MA, van de Weerdt BC, Vader G, et al. Polo-like kinase-1 is required for bipolar spindle formation but is dispensable for anaphase promoting complex/Cdc20 activation and initiation of cytokinesis. J Biol Chem 2004;279:36841–54.
15. Sumara I, Gimenez-Abian JF, Gerlich D, et al. Roles of polo-like kinase 1 in the assembly of functional mitotic spindles. Curr Biol 2004;14:1712–22.
16. Ahonen LJ, Kallio MJ, Daum JR, et al. Polo-like kinase 1 creates the tension-sensing 3F3/2 phosphoepitope and modulates the association of spindle-checkpoint proteins at kinetochores. Curr Biol 2005;15:1078–89.
17. Wong OK, Fang G, Authors FN, Fang G. Plx1 is the 3F3/2 kinase responsible for targeting spindle checkpoint proteins to kinetochores. J Cell Biol 2005;170:709–19.
18. Kang YH, Park JE, Yu LR, et al. Self-regulated Plk1 recruitment to kinetochores by the Plk1–1 interaction is critical for proper chromosome segregation.[see comment]. Mol Cell 2006;24:409–22.
19. Smith MR, Wilson ML, Hamanaka R, et al. Malignant transformation of mammalian cells initiated by constitutive expression of the polo-like kinase. Biochem Biophys Res Commun 1997;234:397–405.
20. Takai N, Hamanaka R, Yoshimatsu J, Miyakawa I. Polo-like kinases (Plks) and cancer. Oncogene 2005;24:287–91.
21. McInnes C, Mezna M, Fischer PM, Authors FN, Mezna M, Fischer PM. Progress in the discovery of polo-like kinase inhibitors. [Review] [161 refs]. Curr Top Med Chem 2005;5:181–97.
22. McInnes C, Mazumdar A, Mezna M, et al. Inhibitors of Polo-like kinase reveal roles in spindle-pole maintenance. Nat Chem Biol 2006;2:608–17.
23. Peters U, Cherian J, Kim JH, et al. Probing cell-division phenotype space and Polo-like kinase function using small molecules. Nat Chem Biol 2006;2:618–26.
24. Hofheinz R, Hochhaus A, Al-Batran S, et al. A phase I repeated dose escalation study of the Polo-like kinase 1 inhibitor BI 2536 in patients with advanced solid tumours. J Clin Oncol (Meeting Abstracts) 2006;24:2038.
25. Munzert G, Steinbild S, Frost A, et al. A phase I study of two administration schedules of the Polo-like kinase 1 inhibitor BI 2536 in patients with advanced solid tumors. J Clin Oncol (Meeting Abstracts) 2006;24:3069.
26. Ohnuma T, Cho SY, Roboz J, et al. Phase I study of ON 01910.Na by 3-day continuous infusion (CI) in patients (pts) with advanced cancer. J Clin Oncol (Meeting Abstracts) 2006;24:13137.
27. Donehower RC, Jimeno A, Li J, et al. Phase I study of ON-01910.Na, a novel cell cycle inhibitor in adult patients with solid tumors. J Clin Oncol (Meeting Abstracts) 2006;24:13026.
28. Steegmaier M, Hoffmann M, Baum A, et al. BI 2536, a potent and selective inhibitor of polo-like kinase 1, inhibits tumor growth *in vivo*. Curr Biol 2007;17:316–22.
29. Lenart P, Petronczki M, Steegmaier M, et al. The small-molecule inhibitor BI 2536 reveals novel insights into mitotic roles of polo-like kinase 1. Curr Biol 2007;17:304–15.
30. Yung-Chi C, Prusoff WH. Relationship between the inhibition constant (KI) and the concentration of inhibitor which causes 50 per cent inhibition (I50) of an enzymatic reaction. Biochem Pharmacol 1973;22:3099–108.
31. Lansing TJ, McConnell RT, Duckett DR, et al. *In vitro* biological activity of a novel small-molecule inhibitor of polo-like kinase 1. Mol Cancer Ther 2007;6:450–9.
32. Emmitte KA, Andrews CW, Badiang JG, et al. Discovery of thiophene inhibitors of polo-like kinase. Bioorg Med Chem Lett 2009;19:1018–21.
33. Spankuch-Schmitt B, Wolf G, Solbach C, et al. Downregulation of human polo-like kinase activity by antisense oligonucleotides induces growth inhibition in cancer cells. Oncogene 2002;21:3162–71.
34. Cogswell JP, Brown CE, Bisi JE, et al. Dominant-negative polo-like kinase 1 induces mitotic catastrophe independent of cdc25C function. Cell Growth Diff 2000;11:615–23.
35. Spankuch-Schmitt B, Bereiter-Hahn J, Kaufmann M, et al. Effect of RNA silencing of polo-like kinase-1 (PLK1) on apoptosis and spindle formation in human cancer cells. J Natl Cancer Inst 2002;94:1863–77.
36. Nousiainen M, Silljé HHW, Sauer G, Nigg EA, Körner R. Phosphoproteome analysis of the human mitotic spindle. 2006;103:5391–6.
37. Gascoigne KE, Taylor SS. Cancer cells display profound intra- and interline variation following prolonged exposure to antimitotic drugs. Cancer Cell 2008;14:111–22.
38. Tao W, South VJ, Zhang Y, et al. Induction of apoptosis by an inhibitor of the mitotic kinesin KSP requires both activation of the spindle assembly checkpoint and mitotic slippage. Cancer Cell 2005;8:49–59.
39. Rieder CL, Maiato H. Stuck in Division or passing through: what happens when cells cannot satisfy the spindle assembly checkpoint. Dev Cell 2004;7:637–51.
40. Weaver BAA, Cleveland DW. Decoding the links between mitosis, cancer, and chemotherapy: the mitotic checkpoint, adaptation, and cell death. Cancer Cell 2005;8:7–12.
41. Lanni JS, Jacks T. Characterization of the p53-dependent postmitotic checkpoint following spindle disruption. Mol Cell Biol 1998;18:1055–64.
42. Margolis RL, Lohez OD, Andreassen PR. G_1 tetraploidy checkpoint and the suppression of tumorigenesis. J Cell Biochem 2003;88:673–83.
43. Gizatullin F, Yao Y, Kung V, Harding MW, Loda M, Shapiro GI. The Aurora kinase inhibitor VX-680 induces endoreduplication and apoptosis preferentially in cells with compromised p53-dependent postmitotic checkpoint function. Cancer Res 2006;66:7668–77.
44. Vijapurkar U, Wang W, Herbst R. Potentiation of kinesin spindle protein inhibitor-induced cell death by modulation of mitochondrial and death receptor apoptotic pathways. Cancer Res 2007;67:237–45.
45. Tao W, South VJ, Diehl RE, et al. An inhibitor of the kinesin spindle protein activates the intrinsic apoptotic pathway independently of p53 and *de novo* protein synthesis. Mol Cell Biol 2007;27:689–98.
46. Shoemaker AR, Oleksijew A, Bauch J, et al. A small-molecule inhibitor of Bcl-XL potentiates the activity of cytotoxic drugs *in vitro* and *in vivo*. Cancer Res 2006;66:8731–9.